Article

B(CF)- vs Al(CF)-Derived Metallocenium Ion Pairs. Structural, Thermochemical, and Structural Dynamic Divergences

Nicholas G. Stahl, Michael R. Salata, and Tobin J. Marks

J. Am. Chem. Soc., **2005**, 127 (31), 10898-10909• DOI: 10.1021/ja0429622 • Publication Date (Web): 15 July 2005

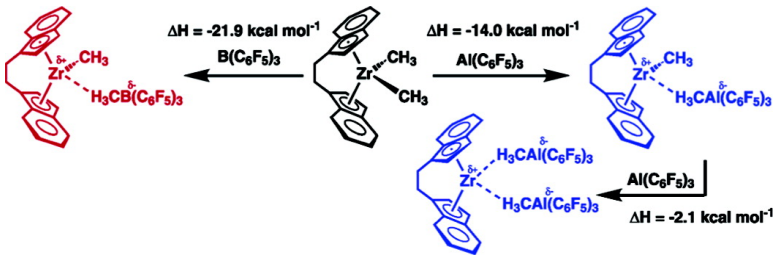

More About This Article

Additional resources and features associated with this article are available within the HTML version:

- Supporting Information
- Links to the 6 articles that cite this article, as of the time of this article download
- Access to high resolution figures
- Links to articles and content related to this article
- Copyright permission to reproduce figures and/or text from this article

View the Full Text HTML

J|A|C|S
ARTICLES
Published on Web 07/15/2005

$B(C_6F_5)_3$- vs $Al(C_6F_5)_3$-Derived Metallocenium Ion Pairs. Structural, Thermochemical, and Structural Dynamic Divergences

Nicholas G. Stahl, Michael R. Salata, and Tobin J. Marks*

Contribution from the Department of Chemistry, Northwestern University, Evanston, Illinois 60208-3113

Received November 22, 2004; E-mail: t-marks@northwestern.edu

Abstract: The thermodynamic and structural characteristics of $Al(C_6F_5)_3$-derived vs $B(C_6F_5)_3$-derived group 4 metallocenium ion pairs are quantified. Reaction of 1.0 equiv of $B(C_6F_5)_3$ or 1.0 or 2.0 equiv of $Al(C_6F_5)_3$ with *rac*-$C_2H_4(\eta^5\text{-Ind})_2Zr(CH_3)_2$ (*rac*-(EBI)$Zr(CH_3)_2$) yields *rac*-(EBI)$Zr(CH_3)^+H_3CB(C_6F_5)_3^-$ (**1a**), *rac*-(EBI)-$Zr(CH_3)^+H_3CAl(C_6F_5)_3^-$ (**1b**), and *rac*-(EBI)$Zr^{2+}[H_3CAl(C_6F_5)_3]^-_2$ (**1c**), respectively. X-ray crystallographic analysis of **1b** indicates the $H_3CAl(C_6F_5)_3^-$ anion coordinates to the metal center via a bridging methyl in a manner similar to $B(C_6F_5)_3$-derived metallocenium ion pairs. However, the $Zr-(CH_3)_{bridging}$ and $Al-(CH_3)_{bridging}$ bond lengths of **1b** (2.505(4) Å and 2.026(4) Å, respectively) indicate the methyl group is less completely abstracted in **1b** than in typical $B(C_6F_5)_3$-derived ion pairs. Ion pair formation enthalpies (ΔH_{ipf}) determined by isoperibol solution calorimetry in toluene from the neutral precursors are $-21.9(6)$ kcal mol^{-1} (**1a**), $-14.0(15)$ kcal mol^{-1} (**1b**), and $-2.1(1)$ kcal mol^{-1} (**1b**→**1c**), indicating $Al(C_6F_5)_3$ to have significantly less methide affinity than $B(C_6F_5)_3$. Analogous experiments with $Me_2Si(\eta^5\text{-}Me_4C_5)(t\text{-BuN})Ti(CH_3)_2$ indicate a similar trend. Furthermore, kinetic parameters for ion pair epimerization by cocatalyst exchange (ce) and anion exchange (ae), determined by line-broadening in VT NMR spectra over the range 25−75 °C, are $\Delta H^{\ddagger}_{ce} = 22(1)$ kcal mol^{-1}, $\Delta S^{\ddagger}_{ce} = 8.2(4)$ eu, $\Delta H^{\ddagger}_{ae} = 14(2)$ kcal mol^{-1}, and $\Delta S^{\ddagger}_{ae} = -15(2)$ eu for **1a**. Line broadening for **1b** is not detectable until just below the temperature where decomposition becomes significant (∼75−80 °C), but estimation of the activation parameters at 72 °C gives $\Delta H^{\ddagger}_{ce} \approx 22$ kcal mol^{-1}and $\Delta H^{\ddagger}_{ae} \approx 16$ kcal mol^{-1}, consistent with the bridging methide being more strongly bound to the zirconocenium center than in **1a**.

Introduction

It is now clear that the weakly coordinating anions of single-site homogeneous olefin polymerization catalyst ion pairs can play a role nearly as important as that of their cationic metallocenium counterparts.[1,2] Thus, the anions can have substantial effects on the molecular weight, branching, and tacticity of the resulting polyolefins. Since the discovery that $B(C_6F_5)_3$ activates group 4 metallocene alkyls and hydrides for olefin polymerization,[3] there have been numerous efforts to synthesize additional novel Lewis-acidic organoboranes.[4] Efforts in this area have led to a plethora of cocatalysts of widely varying Lewis acidities and abilities to finely tune polymerization activity and polymer microstructural characteristics.[5] However, research into analogous perfluoroarylalanes[6] has been less intense, presumably due to their greater propensity for thermal degradation.

Roesky and co-workers first reported the synthesis of $Al(C_6F_5)_3$, which was isolated and crystallographically characterized as a THF adduct.[7] Cowley and co-workers subsequently showed that $Al(C_6F_5)_3$, when crystallized from benzene or toluene, crystallizes as an arene complex.[8] Initial attempts to

(1) For recent reviews of single-site olefin polymerization, see: (a) Gibson V. C.; Spitzmesser, S. K. *Chem. Rev.* **2003**, *103*, 283. (b) Pedeutour, J.-N.; Radhakrishnan, K.; Cramail, H.; Deffieux, A. *Macromol. Rapid Commun.* **2001**, *22*, 1095. (c) Gladysz, J. A., Ed. *Chem. Rev.* **2000**, *100* (special issue on "Frontiers in Metal-Catalyzed Polymerization"). (d) Marks, T. J., Stevens, J. C., Eds. *Topics Catal.* **1999**, *15*, and references therein. (e) Britovsek, G. J. P.; Gibson, V. C.; Wass, D. F. *Angew. Chem., Int. Ed.* **1999**, *38*, 428. (f) Kaminsky, W.; Arndt, M. *Adv. Polym. Sci.* **1997**, *127*, 144. (g) Bochmann, M. *J. Chem. Soc., Dalton Trans.* **1996**, 255.

(2) For recent examples of catalyst-activator interplay, see: (a) Metz, M. V.; Sun, Y.; Stern, C. L.; Marks, T. J. *Organometallics* **2002**, *21*, 3691 and references therein. (b) Chen, Y.-X.; Kruper, W. J.; Roof, G.; Wilson, D. R. *J. Am. Chem. Soc.* **2001**, *123*, 745. (c) Zhou, J.; Lancaster, S. J.; Walter, D. A.; Beck, S.; Thornton-Pett, M.; Bochmann, M. *J. Am. Chem. Soc.* **2001**, *123*, 223. (d) Chase, P. A.; Piers, W. E.; Patrick, B. O. *J. Am. Chem. Soc.* **2000**, *123*, 223. (d) Chase, P. A.; Piers, W. E.; Patrick, B. O. *J. Am. Chem. Soc.* **2000**, *122*, 12911. (e) Chen, Y.-X.; Marks, T. J. in ref 1b, p 1391. (f) Metz, M. V.; Schwartz, D. J.; Stern, C. L.; Nickias, P. N.; Marks, T. J. *Angew. Chem., Int. Ed.* **2000**, *39*, 1312.

(3) (a) Yang, X.; Stern, C. L.; Marks, T. J. *J. Am. Chem. Soc.* **1994**, *116*, 10015. (b) Yang, X.; Stern, C. L.; Marks, T. J. *J. Am. Chem. Soc.* **1991**, *113*, 3623.

(4) (a) Metz, M. V.; Schwartz, D. J.; Stern, C. L.; Marks, T. J.; Nickias, P. N. *Organometallics* **2002**, *21*, 4159. (b) Chase, P. A.; Piers, W. E.; Patrick, B. O. *J. Am. Chem. Soc.* **2000**, *122*, 12911. (c) Piers, W. E.; Irvine, G. J.; Williams, V. C. *Eur. J. Inorg. Chem.* **2000**, *10*, 2131. (d) Williams, V. C.; Piers, W. E.; Clegg, W.; Elsegood, M. R. J.; Collins, S.; Marder, T. B. *J. Am. Chem. Soc.* **1999**, *121*, 3244. (e) Chen, Y.-X.; Metz, M. V.; Li, L.; Stern, C. L.; Marks, T. J. *J. Am. Chem. Soc.* **1998**, *120*, 6287. (f) Li, L.; Marks, T. J. *Organometallics* **1998**, *17*, 3996.

(5) (a) Chen, M.-C.; Roberts, J. A. S.; Marks, T. J. *J. Am. Chem. Soc.* **2004**, *126*, 4605. (b) Li, H.; Li, L.; Marks, T. J.; Liable-Sands, L.; Rheingold, A. L. *J. Am. Chem. Soc.* **2003**, *125*, 10788.

(6) For recent examples of organoaluminum cocatalysts, see: (a) ref 2e. (b) Chen, M.-C.; Roberts, J. A. S.; Marks, T. J. *Organometallics* **2004**, *23*, 932.

(7) Belgardt, T.; Storre, J.; Roesky, H. W.; Noltemeyer, M.; Schmidt, H.-G. *Inorg. Chem.* **1995**, *34*, 3821.

10.1021/ja0429622 CCC: $30.25

employ $Al(C_6F_5)_3$ in olefin polymerization catalysis seem to have been initially frustrated by the facile decomposition of the ion pairs generated by activation of simple biscyclopentadienyl group 4 metallocene alkyls.[9] Subsequently, Chen and co-workers showed that ion pairs formed with *ansa*-bridged metallocenes (i.e., $Me_2Si(Me_4Cp)(t\text{-BuN})Ti(CH_3)_2$ and *rac*-$Me_2Si(\eta^5\text{-indenyl})_2Zr(CH_3)_2$, **A**) are more stable. Furthermore, $Al(C_6F_5)_3$ was

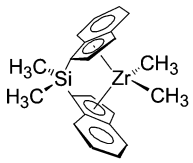

A

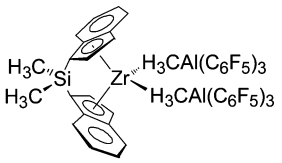

B

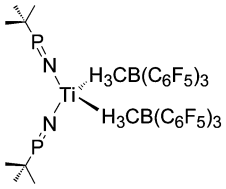

C

shown to abstract *both* metal-bound methide groups from group 4 metallocenes to form diionic species **B**.[2b] The doubly $Al(C_6F_5)_3$-activated metallocenes were found to be more active for olefin polymerization than their monocationic counterparts, and X-ray crystallography confirmed the dianionic nature of the $Al(C_6F_5)_3$ adducts. As far as we are aware, similar behavior for $B(C_6F_5)_3$ has only been crystallographically characterized for a sterically more open nonmetallocene complex, $(^tBu_3PN)_2Ti^{2+}[H_3CB(C_6F_5)_3^-]_2$ (**C**).[10] However, there is spectroscopic evidence for the solution formation of doubly $B(C_6F_5)_3$-activated metallocene complexes as intermediates in intermolecular borane exchange processes.[11]

The origin of the ability of $Al(C_6F_5)_3$ to doubly activate dimethylmetallocenes is not immediately clear. Park and co-workers measured C≡N stretching frequencies of the benzonitrile adducts of $Al(C_6F_5)_3$ and $B(C_6F_5)_3$ and concluded that $Al(C_6F_5)_3$ is considerably less Lewis acidic.[12] However, DFT computational results of Ziegler and co-workers predict that the enthalpy of ion pair formation by methide abstraction from $(1,2\text{-}(CH_3)_2Cp)_2ZrMe_2$ should be -30.8 kcal mol^{-1} for $Al(C_6F_5)_3$ versus only -23.8 kcal mol^{-1} for $B(C_6F_5)_3$[13] ($-24.3(4)$ kcal mol^{-1}, experimental[14]). This result seems inconsistent with a less Lewis acidic nature for $Al(C_6F_5)_3$.

Since its discovery, $Al(C_6F_5)_3$ has been employed as a cocatalyst/activator in the polymerization of ethylene,[15] propylene,[6] 1-hexene,[16] isobutene,[17] methyl methacrylate (MMA),[18] and propylene oxide.[19] Of these, the polymerization of MMA has received considerable attention by Chen and co-workers.[18] $Al(C_6F_5)_3$ not only is active for polymerization but also can dramatically alter resulting polymer microstructural properties. Thus, metallocene-mediated polymerization of MMA with a mixed $B(C_6F_5)_3$ and $Al(C_6F_5)_3$ cocatalyst system has been shown to efficiently produce stereoblock poly-MMA.[18c] Despite the demonstrated competence of $Al(C_6F_5)_3$ as an activator for olefin polymerization and for producing unique polymer microstructures, there is a paucity of data regarding the thermodynamic and kinetic interplay of $Al(C_6F_5)_3$-derived anions with their cationic metallocenium counterparts. In contrast, there is an extensive experimental[14,20] and theoretical[10,21] literature for analogous derivatives of $B(C_6F_5)_3$. If the utility of $Al(C_6F_5)_3$ as a polymerization cocatalyst is to be completely understood and further exploited, kinetic and thermodynamic data will be crucial to understanding catalyst behavior.

To understand the efficacy of $Al(C_6F_5)_3$ to function as a cocatalyst in olefin polymerization, we have undertaken an investigation to quantify its structural, thermochemical, and structural dynamic properties. A series of metallocenium ion pairs, *rac*-$(EBI)Zr(CH_3)^+H_3CB(C_6F_5)_3^-$ (**1a**), *rac*-$(EBI)Zr(CH_3)^+H_3CAl(C_6F_5)_3^-$ (**1b**), and $[rac\text{-}(EBI)Zr]^{2+}[H_3CAl(C_6F_5)_3]_2^-$ (**1c**), has been synthesized, isolated, and purified. Enthalpies

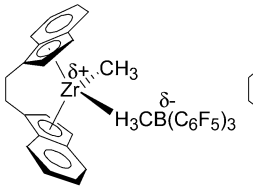

1a

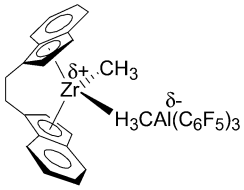

1b

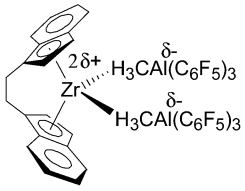

1c

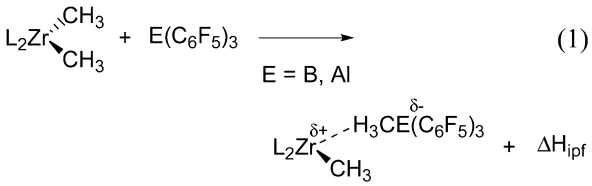

(1)

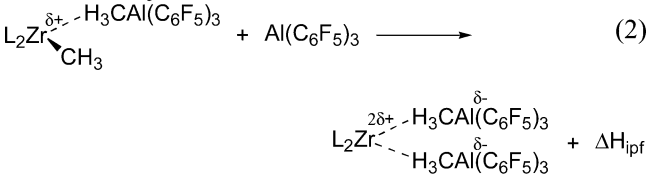

(2)

of reaction for the single methide abstraction from group 4 metallocenes (eq 1) as well as for a second methide abstraction in the case of $Al(C_6F_5)_3$ (eq 2) have been determined in solution by reaction calorimetry. Furthermore, variable-temperature dynamic NMR experiments were conducted to investigate ion

(8) Hair, G. S.; Cowley, A. H.; Jones, R. A.; McBurnett, B. G.; Voigt, A. *J. Am. Chem. Soc.* **1999**, *121*, 4922.
(9) Bochmann, M.; Sarsfield, M. J. *Organometallics* **1998**, *17*, 5908.
(10) Guérin, F.; Stephan, D. W. *Angew. Chem., Int. Ed.* **2000**, *39*, 1298.
(11) (a) Al-Humydi, A.; Garrison, J. C.; Youngs, W. J.; Collins, S. *Organometallics* **2005**, *24*, 193. (b) Green, M. L. H.; Sa*β*mannshausen, J. *Chem. Commun.* **1999**, 115.
(12) Lee, C. H.; Lee, S. J.; Park, J. W.; Kim, K. H.; Lee, B. Y.; Oh, J. S. *J. Mol. Catal. A: Chem.* **1998**, *132*, 231.
(13) Vanka, K.; Chan, M. S. W.; Pye, C. C.; Ziegler, T. *Organometallics* **2000**, *19*, 1841.
(14) Deck, P. A.; Beswick, C. L.; Marks T. J. *J. Am. Chem. Soc.* **1998**, *120*, 1772.
(15) (a) Kim, Y. H.; Kim, T. H.; Kim, N. Y.; Cho, E. S.; Lee, B. Y. *Polym. Prepr. (Am. Chem. Soc., Div. Polym. Chem.)* **2003**, *44*, 990. (b) Kim, Y. H.; Kim, T. H.; Kim, N. Y.; Cho, E. S.; Lee, B. Y. *Polym. Prepr. (Am. Chem. Soc., Div. Poly. Chem.)* **2003**, *44*, 990.

pair structural rearrangement kinetic parameters. It is found that the enthalpy of ion pair methide abstraction/formation associated with $Al(C_6F_5)_3$ is *significantly less* than that of $B(C_6F_5)_3$, and the data as a whole support a picture in which $Al(C_6F_5)_3$ has *significantly less* Lewis acidity and methide affinity than does $B(C_6F_5)_3$.

Experimental Section

Materials and Methods. All manipulations of air-sensitive materials were performed with rigorous exclusion of oxygen and moisture in flamed Schlenk-type glassware on a dual-manifold Schlenk line, interfaced to a high-vacuum line ($<10^{-5}$ Torr), or in a nitrogen-filled MBraun glovebox with a high-efficiency recirculator (<1 ppm O_2 and H_2O). All solvents were freeze−pump−thaw degassed on the high vacuum line, dried over Na/K alloy, and vacuum-transferred to dry storage tubes having PTFE valves. The reagents *rac*-$C_2H_4(\eta^5\text{-Ind})_2ZrMe_2$ (*rac*-(EBI)$ZrMe_2$),[22] $Me_2Si(\eta^5\text{-}Me_4C_5)(t\text{-BuN})TiMe_2$ (CGC-$TiMe_2$),[23] and $Al(C_6F_5)_3\cdot(C_7H_8)_{0.5}$[12] were prepared and purified according to literature methods. **Warning:** *It has been reported in the literature that $Al(C_6F_5)_3$ may explode under thermal or shock conditions that are not well understood.*[7,24] $B(C_6F_5)_3$ was received as a gift from Dow Chemical and was purified by recrystallization from pentane followed by vacuum sublimation at 10^{-5} Torr. The synthesis and isolation of $CGCTiCH_3^+H_3CB(C_6F_5)_3^-$, $CGCTiCH_3^+H_3CAl(C_6F_5)_3^-$,[2b] and $CGCTi^{2+}[H_3CMeAl(C_6F_5)_3]^-{}_2$[2b] have been previously described. NMR experiments were performed on a Varian UNITYInova 500 MHz or a Mercury 400 MHz spectrometer. ^1H and ^{13}C NMR spectra are referenced internally to the solvent resonance. ^{19}F NMR spectra are referenced externally to $CFCl_3$ in $CDCl_3$. Elemental analyses were performed by Midwest Microlab, LLC (Indianapolis, Indiana).

Synthesis of *rac*-(EBI)$ZrCH_3^+H_3CB(C_6F_5)_3^-$ (1a). The reagents *rac*-(EBI)$Zr(CH_3)_2$ (30.0 mg, 79.4 μmol) and $B(C_6F_5)_3$ (40.7 mg, 79.4 μmol, 1.00 equiv) were loaded into a flip-frit apparatus, which was then interfaced to the high-vacuum line. Dry toluene (approximately 25 mL) was condensed in under vacuum in a dry ice/acetone bath. The cold bath was removed and the solution allowed to warm to 25 °C while stirring, yielding a bright yellow solution. Sufficient toluene was then removed in vacuo until the ion pair complex began to precipitate. Removal of solvent was then halted, and the solution was warmed slightly to redissolve the precipitate. The solution was next slowly recooled, and pentane (approximately 25 mL) was condensed in under vacuum. The bright yellow product was precipitated with stirring, filtered, and dried in vacuo (10^{-6} Torr). Isolated yield: 35.8 mg (51%). The NMR spectroscopic data are consistent with those of similar ion pairs.[25] ^1H (C_6D_6, rt): δ 7.33 (d, 1H), 6.95 (dd, 1H), 6.88 (d, 1H), 6.77 (d, 1H), 6.66 (dd, 1H), 6.57 (d, 1H), 6.31 (dd, 1H), 6.23 (m, 2H), 5.91 (d, 1H), 5.58 (d, 1H), 5.08 (d, 1H), 2.69−2.62 (br m, 1H), 2.50−2.47 (br m, 2H), 2.38−2.33 (br m, 1H), −0.44 (s, 3H), −0.62 (br d, 3H). $^{13}C\{^1H\}$ (C_6D_6, rt): δ 127.4, 127.2, 127.0, 126.5, 125.0, 123.2, 121.4, 116.1, 112.8, 110.5, 104.6, 47.6, 28.8, 27.5. ^{19}F (C_6D_6, rt): δ −134.0 (m, 6 F, *o*-F), −159.7 (m, 3 F, *p*-F), −164.8 (m, 6 F, *m*-F). Anal. Calcd for $C_{40}H_{22}BF_{15}Zr$: C, 54.00; H, 2.49. Found: C, 54.21, 54.25; H, 2.79, 2.86.

Synthesis of *rac*-(EBI)$ZrCH_3^+H_3CAl(C_6F_5)_3^-$ (1b). The reagents *rac*-(EBI)$Zr(CH_3)_2$ (30.0 mg, 79.4 μmol) and $Al(C_6F_5)_3\cdot(C_7H_8)_{0.5}$ (45.6 mg, 79.4 μmol, 1.00 equiv) were loaded into a flip-frit apparatus, which was then interfaced to the high-vacuum line. Dry pentane (approximately 25 mL) was condensed in under vacuum in a dry ice/acetone bath. The cold bath was then removed, and the solution allowed to warm to 25 °C while stirring to provide a bright yellow precipitate. The product was collected by filtration and dried in vacuo (10^{-6} Torr). Isolated yield: 40.3 mg (56%). The NMR spectroscopic data are consistent with those of similar ion pairs.[25] ^1H (C_6D_6, rt): δ 7.37 (d, 1H), 6.98 (m, 2H), 6.81 (d, 1H), 6.70 (dd, 1H), 6.63 (d, 1H), 6.42 (t, 1H), 6.34 (dd, 1H), 6.23 (d, 2H), 5.59 (d, 1H), 5.10 (d, 1H), 2.75−2.681 (br m, 1H), 2.57−2.47 (br m, 2H), 2.43−2.38 (br m, 1H), −0.66 (s, 3H), −1.110 (s, 3H). $^{13}C\{^1H\}$ (C_6D_6, rt): δ 128.7, 127.4, 127.2, 127.1, 126.9, 126.3, 125.0, 123.2, 121.6, 115.6, 113.0, 109.8, 106.0, 47.0, 28.2, 27.7. ^{19}F (C_6D_6, rt): δ −123.2 (d, 6 F, *o*-F), −154.4 (t, 3 F, *p*-F), −162.2 (m, 6 F, *m*-F). Anal. Calcd for $C_{40}H_{22}AlF_{15}Zr$: C, 53.04; H, 2.45. Found: C, 52.85; H, 2.66.

Synthesis of *rac*-(EBI)$Zr^{2+}[(CH_3)Al(C_6F_5)_3^-]_2$ (1c). Ion pair complex **1c** was prepared in a manner similar to **1a**. The reagents *rac*-(EBI)$Zr(CH_3)_2$ (30.0 mg, 79.4 μmol) and $Al(C_6F_5)_3\cdot(C_7H_8)_{0.5}$ (95.8 mg, 167 μmol, 2.10 equiv) were loaded into a flip-frit apparatus, which was then interfaced to the high-vacuum line. Dry toluene (approximately 25 mL) was condensed in under vacuum in a dry ice/acetone bath. The cold bath was next removed and the solution allowed to warm to 25 °C while stirring, yielding a deep red solution. Sufficient toluene was then removed in vacuo until the ion pair complex began to precipitate. Removal of solvent was then halted, and the solution was warmed slightly to redissolve the precipitate. The solution was next slowly recooled and pentane (approximately 25 mL) was condensed in under vacuum. The deep red product was precipitated with stirring, filtered, and dried in vacuo (10^{-6} Torr). Isolated yield: 73.4 mg (49%). ^1H (C_6D_6, rt): δ 6.38 (d, 8.4 Hz, 2H), 6.24 (app. s, 2H), 5.37 (app. s, 2H), 2.67 (d, 8.4 Hz, 2H), 2.43 (d, 8.4 Hz, 2H), −0.55 (s, 6H). ^{19}F (C_6D_6, rt): δ −123.6 (d, 6 F, *o*-F), −152.0 (t, 3 F, *p*-F), −161.3 (m, 6 F, *m*-F). This compound is too insoluble in benzene-d_6 to obtain a ^{13}C NMR spectrum. Anal. Calcd for $C_{58}H_{22}Al_2F_{30}Zr$: C, 48.58; H, 1.55. Found: C, 48.62; H, 1.80.

Solution Reaction Calorimetry. To ensure that the reactions used for calorimetry studies are rapid, clean, and quantitative, ion pair formation reactions were investigated by ^1H NMR in benzene-d_6. A precisely measured amount of *rac*-(EBI)$Zr(CH_3)_2$ or CGCTi$(CH_3)_2$ was added to a septum-capped NMR tube, and the ^1H NMR spectrum was acquired. Next, benzene-d_6 solutions of either $B(C_6F_5)_3$ or $Al(C_6F_5)_3$ of accurately known concentration were added incrementally to the tube in 0.2 molar equiv. The sample was shaken after each addition to ensure mixing, and the NMR spectrum was then measured after each addition.

Reaction calorimetry was carried out using a model 4300 Isoperibol solution calorimeter supplied by Calorimetry Sciences Corporation,

(16) Landis, C. R.; Rosaaen, K. A.; Uddin, J. *J. Am. Chem. Soc.* **2002**, *124*, 12062.
(17) Kumar, K. R.; Hall, C.; Penciu, A.; Drewitt, M. J.; McInenly, P. J.; Baird, M. C. *J. Polym. Sci., Part A: Polym. Chem.* **2002**, *40*, 3302.
(18) (a) Jin, J.; Mariott, W. R.; Chen, E. Y.-X. *J. Polym. Sci., Part A: Polym. Chem.* **2003**, *41*, 3132. (b) Chen, E. Y. X.; Cooney, M. J. *J. Am. Chem. Soc.* **2003**, *125*, 7150. (c) Bolig, A. D.; Chen, E. Y.-X. *J. Am. Chem. Soc.* **2002**, *124*, 5612. (d) Bolig, A. D.; Chen, E. Y.-X. *J. Am. Chem. Soc.* **2001**, *123*, 7943.
(19) Chakraborty, D.; Rodriguez, A.; Chen, E. Y.-X. *Macromolecules* **2003**, *36*, 5470.
(20) (a) Beswick, C. L.; Marks, T. J. *J. Am. Chem. Soc.* **2000**, *122*, 10358 and references therein. (b) Beck, S.; Lieber, S.; Schaper, F.; Geyer, A.; Brintzinger, H.-H. *J. Am. Chem. Soc.* **2001**, *123*, 1483. (c) There should be minimal ion pair aggregation under these conditions: Zuccaccia, C.; Stahl, N. G.; Macchioni, A.; Chen, M.-C.; Roberts, J. A.; Marks, T. J. *J. Am. Chem. Soc.* **2004**, *126*, 1448.
(21) (a) Xu, Z.; Vanka, K.; Ziegler, T. *Organometallics* **2004**, *23*, 104. (b) Xu, Z.; Vanka, K.; Firman, T.; Michalak, A.; Zurek, E.; Zhu, C.; Ziegler, T. *Organometallics* **2002**, *21*, 2444. (c) Lanza, G.; Fragalà, I. L.; Marks, T. J. *Organometallics* **2002**, *21*, 5594. (d) Lanza, G.; Fragalà, I. L.; Marks, T. J. *J. Am. Chem. Soc.* **2000**, *122*, 12764. (e) Chan, M. S. W.; Ziegler, T. *Organometallics* **2000**, *19*, 5182. (f) Chan, M. S. W.; Vanka, K.; Pye, C. C.; Ziegler, T. *Organometallics* **1999**, *18*, 4624.
(22) Chien, J. C. W.; Tsai, W. M.; Rausch, M. D. *J. Am. Chem. Soc.* **1991**, *113*, 8570.
(23) (a) Stevens, J. C.; Timmers, F. J.; Wilson, D. R.; Schmidt, G. F.; Nickias, P. N.; Rosen, R. K.; Knight, G. W.; Lai, S. Y. (Dow Chemical Co.) *Constrained Geometry Addition Polymerization Catalysts, Processes for Their Preparation, Precursors Therefore, Methods of Use, and Novel Polymers Formed Therewith*; EP0416815, Mar 13, 1991. (b) Canich, J. M.; Hlatky, G. G.; Turner, H. W. (Exxon Chemical Patents, Inc.) *Aluminum-Free Monocyclopentadienyl Metallocene Catalysts for Olefin Polymerization*; WO-9200333 A2, Jan 9, 1992. (c) Canich, J. A. M. (Exxon Chemical Patents, Inc.) *Olefin Polymerization Catalysts*; EP-420436A1, April 3, 1991.
(24) (a) Pohlmann, J. L. W.; Brinckmann, F. E. *Z. Naturforsch. B* **1965**, *20b*, 5. (b) Chambers, R. D. *Organomet. Chem. Rev.* **1966**, *1*, 279.
(25) Bolig, A. D.; Chen, E. Y.-X. *J. Am. Chem. Soc.* **2004**, *126*, 4897.

which was extensively modified in-house for use with extremely air- and water-sensitive reagents. A computer interfaced to the calorimeter controlled the experiment and logged thermochemical data.

In a typical titration experiment used to measure the heats of methide abstraction, the metallocene was weighed into an individual ampule and interfaced to the calorimeter. In the case of experiments measuring the second methide abstraction enthalpy, 1.0 molar equiv of $Al(C_6F_5)_3 \cdot (C_7H_8)_{0.5}$ was weighed into a second ampule and was also interfaced to the calorimeter. Borane/alane titrant solution and solvent were next charged into the appropriate calorimeter storage vessels and interfaced to the calorimeter. The system was then evacuated and backfilled three times with argon and evacuated at 10^{-6} Torr for at least 6.0 h to remove any traces of water and oxygen. The masses of the reagents were chosen so as to provide approximately 0.5×10^{-3} M solutions of reagents in the reaction vessel. After evacuation, the titrant was transferred to the calorimeter buret, the solvent was introduced into the reaction dewar, and the metallocene dimethyl ampule was broken into the solvent. Stirring was then initiated, and the apparatus was lowered into a thermostated 25.000 ± 0.002 °C water bath. The calorimeter constant was determined using a calibrated resistor heater, and this procedure was carried out before each titration. The $Al(C_6F_5)_3$ or $B(C_6F_5)_3$ solution was then injected with the precisely calibrated buret, which was driven by a stepper motor to inject titrant at a constant rate.

Batch addition experiments were used to measure the solvation energies of $Al(C_6F_5)_3$ and $B(C_6F_5)_3$. After evacuation the solvent was introduced into the reaction dewar, stirring was initiated, and the system was calibrated in the same manner as that during a titration experiment. At a predetermined time during the experiment, the ampule containing the cocatalyst was broken into the toluene and the temperature change was monitored.

A precision thermistor monitored the reaction vessel temperature during the course of the experiments. The thermochemical data were corrected and analyzed using the software supplied by Calorimeter Sciences Corporation, which is based on the methods of Eatough, Christensen, and Izatt.[26] In all cases, the reactions were fast and quantitative, allowing a straightforward analysis.

DNMR Studies of Ion Pair Structural Reorganization. In the glovebox, pure *rac*-(EBI)$ZrCH_3^+H_3CB(C_6F_5)_3^-$ and *rac*-(EBI)$ZrCH_3^+H_3CAl(C_6F_5)_3^-$ were loaded into separate Teflon-valved J-Young NMR tubes. Next, 0.80 mL of a 1.0 mM stock solution of Si(*p*-tolyl)$_4$ in benzene-d_6 was added to each tube. Temperatures were varied over the range 25−80 °C. At ∼80 °C, **1a** and **1b** begin to decompose in solution, making precise determination of the coalescence point impossible. Prior to each data acquisition, the NMR probe was equilibrated at the desired temperature for 15 min. Each spectrum was acquired as 6701 points over a range of 6689 Hz and then zero-filled to 65 536 points (resolution = 0.10 Hz). Unweighted Fourier transforms of each FID were phased carefully and subjected to drift and baseline corrections as well as reference deconvolution on the methyl resonance of Si(*p*-tolyl)$_4$ as the internal line shape standard using the Hilbert algorithm,[27] such that the final standard peak width was 3.00 Hz in all spectra. Resonance broadening of two diastereotopic protons on the indenyl ligand and the nonbridging Zr−Me group were monitored. Due to overlap of the Zr−Me and Zr−Me−B resonances of **1a** at higher temperatures, line widths were measured using line shape simulation implemented in the GNMR software package. Rate constants at each temperature were calculated by measuring the excess line broadening in comparison to the line width in the slow-exchange limit (25 °C). Values and standard deviations for $\Delta H^{\ddagger}$ and $\Delta S^{\ddagger}$ were determined from linear regression analysis of a plot of $\ln(k/T)$ vs $1/T$.

X-ray Crystal Structure Determination. A crystal of $Al(C_6F_5)_3$-containing **1b** suitable for X-ray diffraction was obtained by layering pentane on top of a solution of the ion pair at −30 °C inside a 4 mm glass tube. A crystal was subsequently selected and mounted under Infineum V8512 oil and maintained under a nitrogen cold-stream at 153(2) K for data collection. Diffraction data were obtained using a Bruker SMART 1000 CCD area detector diffractometer with a fine-focus, sealed tube Mo Kα radiation source ($\lambda = 0.710\ 73$ Å) and a graphite monochromator.

The crystal structure was solved by direct methods, and the solution was refined through successive least-squares cycles and subjected to a face-indexed absorption correction. The refinements were carried to convergence with the hydrogen atoms of the bridging methyl group located in the electron difference map, while the remaining hydrogen atoms were placed in idealized positions and refined isotropically with fixed U_{eq} under standard riding model constraints. Crystal data collection and refinement parameters are summarized in Table 1 and in the Crystallographic Information File (CIF, see Supporting Information).

Table 1. Summary of the Crystal Structure Data for Complex **1b**[a]

formula	$C_{40}H_{22}AlF_{15}Zr$
formula weight	905.78
crystal color, habit	yellow, block
crystal dimensions, mm^3	0.140× 0.196 × 0.186
crystal system	monoclinic
space group	$P2_1/c$
a, Å	10.6403(13)
b, Å	19.650(3)
c, Å	17.091(2)
β, deg	94.803(2)
V, Å^3	3560.9(8)
Z	4
d (calcd), g cm^{-3}	1.690
μ, mm^{-1}	0.443
$T_{min}-T_{max}$	0.925 52−0.945 38
measured reflections	32158
independent reflections	8667
reflections > 2σ (I)	5901
R_{int}	0.0453
$R[F^2 > 2\sigma(F^2)]$	0.0564
$wR(F^2)$	0.1367
S	1.064
no. of parameters	526

[a] CCD area detector diffractometer; φ and ω scans; temperature for data collection, 153(2) K; Mo Kα radiation; $\lambda = 0.710\ 73$ Å.

Results

The following sections first describe the synthesis and characterization of the products formed by heterolytic abstraction of the methide substituents from *rac*-(EBI)$Zr(CH_3)_2$ and CGCTi-$(CH_3)_2$ by $B(C_6F_5)_3$ and $Al(C_6F_5)_3$. The reactions are examined both by bulk synthesis and isolation as well as by NMR-scale titration-type reactions to confirm their suitability for calorimetric analysis. Characterization includes the crystal structure determination of **1b** and comparison of the derived structural parameters with those of comparable boron and aluminum compounds. The ion pair formation enthalpies are measured by titration of *rac*-(EBI)$ZrMe_2$ directly with $B(C_6F_5)_3$ or $Al(C_6F_5)_3$. Finally, the kinetics of ion pair structural reorganization are analyzed.

Synthesis of Ion Pairs. The synthesis of $B(C_6F_5)_3$ and Al-$(C_6F_5)_3$ adducts is straightforward. For single methide abstraction by $B(C_6F_5)_3$ (**1a**) and double methide abstraction by $Al(C_6F_5)_3$ (**1c**), the reaction with *rac*-(EBI)$ZrMe_2$ proceeds cleanly in toluene. Both products are relatively soluble in toluene (up to approximately 50 mM for **1a** and approximately 20 mM for **1c**), and addition of pentane completely precipitates the ion pair complexes. However, in the case of complex **1b**, it is sufficient

(26) Eatough, D. J.; Christensen, J. J.; Izatt, R. M. *Experiments in Thermometric Titrimetry and Titration Calorimetry*; Brigham Young University Press: Provo, Utah, 1974.
(27) Rutledge, D. N., Ed. *Signal Treatment and Signal Analysis in NMR*; Elsevier Science: New York, 2003; Chapter 16.

to combine *rac*-(EBI)Zr(CH_3)$_2$ and Al(C_6F_5)$_3$·(C_7H_8)$_{0.5}$ in pentane only. Complex **1b** is considerably more soluble in toluene and difficult to precipitate even with the addition of large amounts of pentane, suggesting greater covalent character. Filtration of the reaction solutions affords powders, which, when stored at −40 °C in the dark in a glovebox, are stable for periods of at least several months. When the reactions are performed in septum-capped NMR tubes, the measured spectra indicate complete and quantitative formation of the ion pairs within the time required to inject an aliquot of cocatalyst and acquire the ^{1}H NMR spectrum (∼1 min). Indeed, solution reaction calorimetry shows the reactions to be nearly instantaneous (vide infra).

Reaction of Ion Pairs with THF. As expected, reaction of B(C_6F_5)$_3$-derived **1a** with 1.0 equiv of THF effects displacement of the $H_3CB(C_6F_5)_3^-$ anion generating *rac*-(EBI)Zr(CH_3)(THF)$^+$ $H_3CB(C_6F_5)_3^-$ as judged by NMR (eq 3). In contrast, reaction

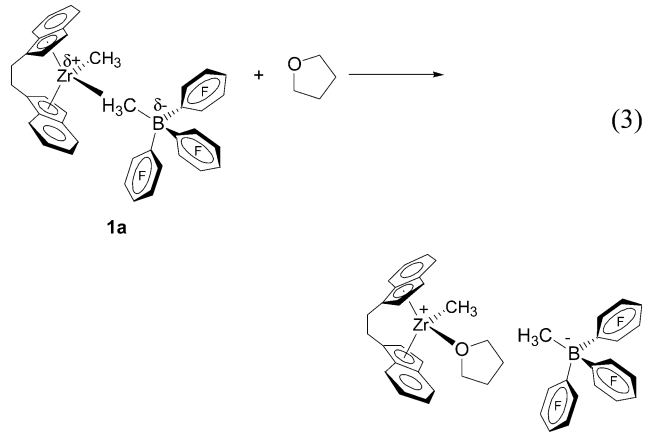

(3)

1a

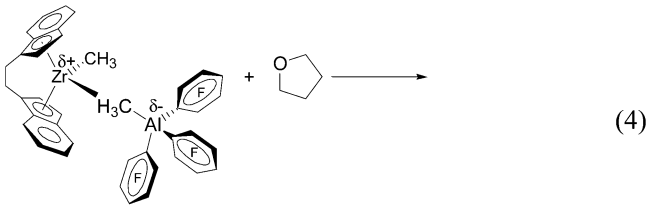

(4)

1b

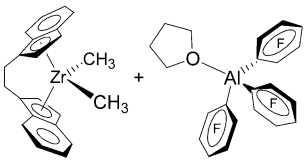

of Al(C_6F_5)$_3$-derived **1b** with THF *does not* effect anion displacement. Rather, the resonances in the ^{1}H NMR spectrum associated with the metallocene ligand indicate that the neutral dimethylmetallocene species is regenerated, and the ^{1}H and ^{19}F NMR spectra indicate the formation of the known THF−Al(C_6F_5)$_3$ adduct (eq 4).[7,18a,18c,28]

Crystal Structure of 1b. A single crystal of **1b** suitable for X-ray diffraction analysis was obtained by diffusion of pentane into a toluene solution of **1b** at −30 °C. Unfortunately, attempts to isolate diffraction quality single crystals of **1a** and **1c** were unsuccessful. Selected bond distances and angles of **1b** are presented in Table 2, and an ORTEP representation is shown in Figure 1.

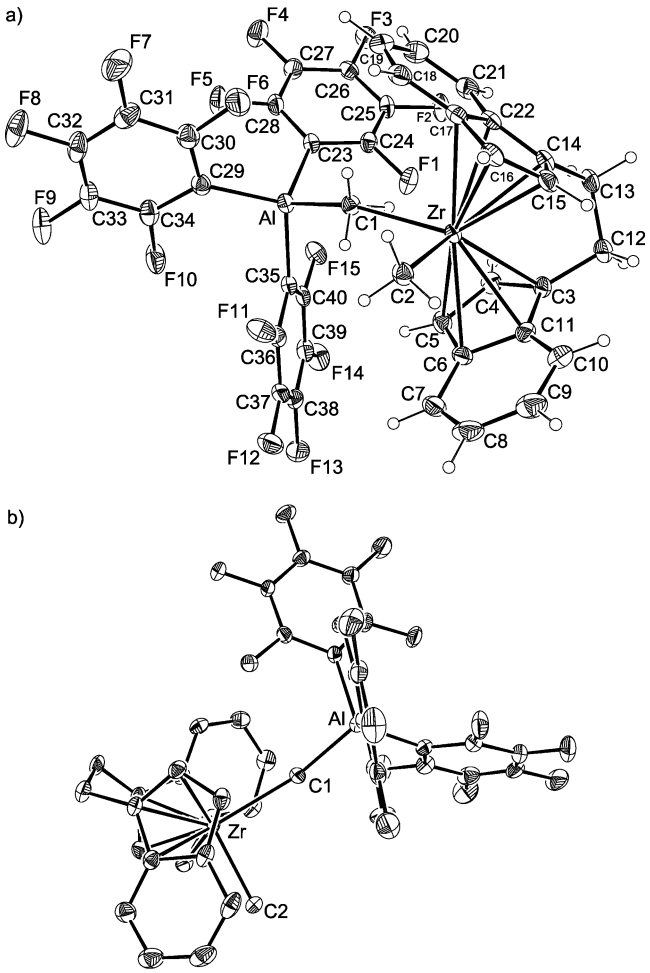

Figure 1. ORTEP drawings of the molecular structure of the complex [(CH_2CH_2)Ind$_2$]ZrMe$^+$ MeAl(C_6F_5)$_3^-$ (**1b**). (a) "Side" view with all atoms pictured. (b) "Top" view in which hydrogen atoms have been omitted for clarity. Thermal ellipsoids are drawn at the 30% probability level in both drawings.

To a first approximation, the $H_3CAl(C_6F_5)_3^-$ anion adopts a similar coordination geometry to that of B(C_6F_5)$_3$-derived ion pairs. The pentafluorophenyl groups on aluminum adopt a pinwheel-type conformation, and the anion coordinates to the metal center via the abstracted methide. The hydrogen atoms on the bridging CH_3 were located in the electron difference map, and their positions indicate them to be pointing away from the aluminum and toward the zirconocenium cation. The Zr−$CH_{3(terminal)}$ bond length is 2.252(3) Å, while the Zr−$CH_{3(bridging)}$ bond length is 2.505(4) Å, an indication that it has indeed been abstracted to some significant degree from the zirconium. As in the case of B(C_6F_5)$_3$-derived ion pairs, the Zr−H_3C−Al angle is near linear at 160.3(2)° and the $H_3C_{(bridging)}$−Zr−$CH_{3(terminal)}$ bond angle is 93.25(13)°. Analysis of close nonbonded contacts indicates that steric crowding is not very prominent. Comparisons to the structures of related ion pairs are made in the Discussion section.

Enthalpies of Ion Pair Formation. The enthalpies of ion pair formation, as described by eqs 1 and 2, were determined by titrating solutions of either B(C_6F_5)$_3$ or Al(C_6F_5)$_3$ into toluene solutions of the metallocene dimethyls within an anaerobic solution reaction isoperibol calorimeter. While in previous

(28) Jin, J.; Chen, E. Y.-X. *Organometallics* **2002**, *21*, 13.

Table 2. Selected Bond Distances (Å) and Angles (deg) for Complex **1b**

Bond Distances (Å)							
Al−C1	2.026(4)	Zr−C1	2.505(4)	Zr−C2	2.252(3)	Zr−Cp(1)	2.198
Zr−Cp(2)	2.211	Zr−C3	2.482(4)	Zr−C4	2.464(3)	Zr−C5	2.519(4)
Zr−C6	2.595(4)	Zr−C11	2.539(4)	Zr−C14	2.454(3)	Zr−C15	2.467(3)
Zr−C16	2.519(4)	Zr−C17	2.578(4)	Zr−C22	2.529(4)	C3−C12	1.506(5)
C12−C13	1.515(6)	C13−C14	1.508(5)	Al−C23	2.010(4)	Al−C29	2.000(4)
Al−C35	2.020(4)						

Bond Angles (deg)			
Al−C1−Zr	160.3(2)	C1−Zr−C2	93.25(13)
C1−Al−C23	107.51(15)	C1−Al−C29	112.37(16)
C1−Al−C35	104.82(16)	C23−Al−C29	111.59(15)
C23−Al−C35	109.07(15)	C29−Al−C35	111.16(16)
C3−Zr−C14	69.23(12)	Zr−C14−C13	114.7(2)
C14−C13−C12	110.4(3)	C13−C12−C3	110.5(3)
C12−C3−Zr1	116.7(3)		

Table 3. Ion Pair Formation Enthalpies (ΔH_{ipf}) in Toluene Solution at 25 °C for Metallocene Methide Abstraction by $E(C_6F_5)_3$ (E = B, Al) Organo-Lewis Acid Reagents

entry	metallocene	reagent	ΔH_{ipf} (kcal mol^{-1})	reference
1	*rac*-(EBI)$ZrMe_2$	$B(C_6F_5)_3$	−21.9(6)	this work
2	*rac*-(EBI)$ZrMe_2$	$Al(C_6F_5)_3$, 1st eq	−14.0(1.5)	this work
3	*rac*-(EBI)$ZrMe_2$	$Al(C_6F_5)_3$, 2nd eq	−2.1(1)	this work
4	$CGCTiMe_2$	$B(C_6F_5)_3$	−22.6(2)	20
5	$CGCTiMe_2$	$Al(C_6F_5)_3$, 1st eq	−13.9(6)	this work
6	$CGCTiMe_2$	$Al(C_6F_5)_3$, 2nd eq	−3.4(8)	this work
7	Cp_2ZrMe_2	$B(C_6F_5)_3$	−23.1(3)	20
8	(1,2-Me_2Cp)$ZrMe_2$	$B(C_6F_5)_3$	−24.3(4)	20
9	$CGCZrMe_2$	$B(C_6F_5)_3$	−23.9(4)	20

similar calorimetric studies,[20a,b] dialkylmetallocenes were titrated into solutions of borane activator, the double activating ability of $Al(C_6F_5)_3$ necessitates performing the titration in the reverse direction. In this way it is possible to isolate the thermochemical events in which $Al(C_6F_5)_3$ abstracts a second methide group from those in which a single methide is abstracted. ^{1}H NMR experiments in which the borane and alane activators were introduced into solutions containing an excess of metallocene dimethyl afford net results equivalent to those in which the metallocene dimethyl is introduced into an excess of the activator. In all cases, the reactions are found to be clean, quantitative, and rapid. No significant species other than the product ion pair complexes of interest are observable in the ^{1}H NMR spectrum. In addition, the thermograms generated during calorimetry experiments indicate that heat evolution begins almost immediately after the titration begins and that heat evolution ceases almost immediately after the titration ends, indicating a nearly instantaneous reaction.

Thermochemical data for a series of ion pair formation reactions are presented in Table 3. As can be readily seen, the abstraction of methide by $Al(C_6F_5)_3$ is 8−9 kcal mol^{-1} *less exothermic* than abstraction by $B(C_6F_5)_3$ for both *rac*-(EBI)Zr-$(CH_3)_2$ and $CGCTi(CH_3)_2$. The second methide abstraction by $Al(C_6F_5)_3$, at −2.1(1) kcal mol^{-1} for *rac*-(EBI)$Zr(CH_3)_2$ and −3.4(8) kcal mol^{-1} for $CGCTi(CH_3)_2$, is only modestly exothermic. The heats of solvation (ΔH_{solv}) of $B(C_6F_5)_3$ and $Al(C_6F_5)_3{\cdot}(C_7H_8)_{0.5}$ in toluene were measured and found to be +5.5(3) kcal mol^{-1} and +2.9(1) kcal mol^{-1}, respectively. As can be seen, mild endothermicity is observed for dissolution of both compounds, with that of $Al(C_6F_5)_3{\cdot}(C_7H_8)_{0.5}$ being about 2.6 kcal mol^{-1} less endothermic than that of $B(C_6F_5)_3$.

Ion Pair Structural Reorganization Processes. There are two spectroscopically differentiable structural rearrangement processes by which the anionic moiety can migrate from one side of the zirconocenium-methyl center to the other (i.e., stereoinversion of the ion pair).[14,20] In one rearrangement process, the methyl-borate/aluminate anion formally migrates from one side of the metallocene framework to the other (anion exchange, ae; eq 5; note that the ethylene bridges have been removed from the schematic structures for clarity). In this

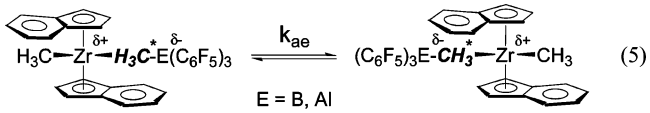

(5)

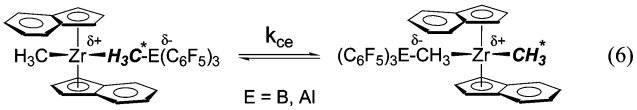

(6)

process, the EBI ligand nuclei undergo site exchange and thus broaden and should ultimately collapse/coalesce in the variable-temperature ^{1}H NMR spectrum, whereas the terminal and bridging $Zr-CH_3$ groups retain their identity and do not undergo broadening due to this process. The other possible rearrangement process is the formal exchange (in principle either intra- or intermolecular) of the neutral borane/alane cocatalyst molecule from one side of the metallocenium moiety to the other (cocatalyst exchange, ce; eq 6). In this process, both the indenyl ligand nuclei and the terminal and bridging methide groups undergo site exchange leading to broadening of all resonances in the ^{1}H NMR spectrum. Thus, the rate of the various dynamic processes can be directly determined by measuring the line broadening associated with the bridging and terminal methide signals. Subtracting this rate from the overall rate of exchange associated with the other resonances yields the frequently more rapid[14,20] rate of anion exchange.

The results of the dynamic NMR experiments are presented in Table 4. For $B(C_6F_5)_3$-derived **1a**, anion exchange proceeds with activation parameters $\Delta H_{ae}^{\ddagger} = 14(2)$ kcal mol^{-1} and $\Delta S_{ae}^{\ddagger} = -15(2)$, and cocatalyst exchange proceeds with activation parameters $\Delta H_{ce}^{\ddagger} = 22(1)$ kcal mol^{-1} and $\Delta S_{ce}^{\ddagger} = 8(2)$, indicating that anion exchange is the dominant (lower activation energy) process contributing to line-broadening under these conditions. These data indicate that cocatalyst exchange proceeds with $\Delta G_{ce}^{\ddagger} = 19.6$ kcal mol^{-1} at 25 °C and are in good agreement with the value $\Delta G_{ce}^{\ddagger} = 18.4$ kcal mol^{-1} reported

Table 4. Kinetic Data for Ion Pair Structural Reorganization Processes Cocatalyst Exchange (ce, Eq 5) and Anion Exchange (ae, Eq 6) in Benzene-d_6

complex	$\Delta H^{\ddagger}_{ce}$ (kcal mol^{-1})	$\Delta S^{\ddagger}_{ce}$ (eu)	$\Delta H^{\ddagger}_{ae}$ (kcal mol^{-1})	$\Delta S^{\ddagger}_{ae}$ (eu)
rac-(EBI)ZrMe$^+$H$_3$CB(C$_6$F$_5$)$_3^-$	22(1.0)	8.2(4)	14(2)	−15(2)
rac-(EBI)ZrMe$^+$H$_3$CAl(C$_6$F$_5$)$_3^-$	∼22		∼16	
(1,2-Me$_2$Cp)$_2$ZrMe$^+$H$_3$CB(C$_6$F$_5$)$_3^-$[a]	27(2)	22(3)	22(1)	13(2)

[a] Provided for comparison (from refs 14, 20).

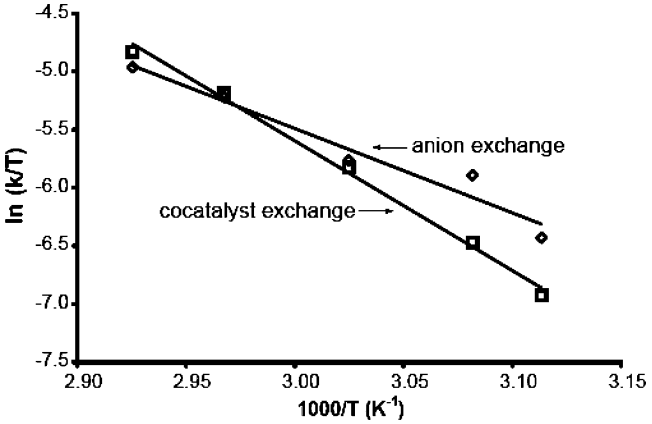

Figure 2. Arrhenius plot for the anion and cocatalyst exchange processes associated with complex **1b** in benzene-d_6.

earlier by Seidle and Newmark.[29] This experiment was performed on both a ∼10 mM and ∼2 mM solution of **1a**, and the activation parameters determined at each concentration are indistinguishable. A plot of ln(k/T) vs 1000/T is shown in Figure 2.

Unfortunately, the resonances of **1b** undergo no significant line broadening until near the temperature at which decomposition makes accurate measurements impossible (∼75−80 °C), rendering accurate determination of the kinetic parameters over a temperature range impossible for this complex. Nonetheless, a small amount of line-broadening is detectable at 72 °C and indicates a cocatalyst exchange rate of ∼5 s^{-1} and an anion exchange rate of ∼0.3 s^{-1}, versus 4.6 s^{-1} and 3.4 s^{-1}, respectively, for **1a** at 72 °C. This thermal instability also precludes accurate determination of rates by 2D-EXSY methods. Reasonably assuming that the entropies of activation for **1b** are approximately the same as those of **1a**, the enthalpies of activation are estimated to be $\Delta H_{ae}^{\ddagger} \approx 16$ kcal mol^{-1} and $\Delta H_{ce}^{\ddagger} \approx 22$ kcal mol^{-1}.

Discussion

The microstructures of the polymeric products formed via single-site polymerization processes are intimately related to the thermodynamic, structural, and structural dynamic characteristics of the catalytic species. Without a quantitative understanding of these characteristics, it is not possible to fully understand how metallocenium ion pairs function in encoding polymer microstructures. In light of recent results indicating the competence of Al(C$_6$F$_5$)$_3$ to function as an effective cocatalyst[15−19] and its unique ability to abstract two methide groups from group 4 metallocenes,[2b] this study was undertaken to determine the thermodynamic and structural properties of Al(C$_6$F$_5$)$_3$-derived metallocenium ion pairs in order to gain a better understanding of the unique properties of Al(C$_6$F$_5$)$_3$ as a cocatalyst. Given the structural and chemical similarities of Al(C$_6$F$_5$)$_3$ and B(C$_6$F$_5$), it is appropriate to compare and contrast the two quantitatively. The data discussed here are representative of both B(C$_6$F$_5$)$_3$-derived and Al(C$_6$F$_5$)$_3$-derived metallocenium ion pairs, and their differences are examined in detail.

Synthesis and Reactivity of Al(C$_6$F$_5$)$_3$- and B(C$_6$F$_5$)$_3$-Derived Ion Pairs. Some understanding of the nature of B(C$_6$F$_5$)$_3$- and Al(C$_6$F$_5$)$_3$-derived ion pairs can be gained in the process of isolating them. It is observed that Al(C$_6$F$_5$)$_3$-derived ion pair **1b** is appreciably soluble in toluene and difficult to precipitate with even large amounts of pentane, whereas the syntheses of **1a** and **1c** can be achieved in toluene, followed by facile precipitation with pentane.[30] That **1b** can be synthesized in neat pentane is also likely a reflection of the reduced polarity of **1b** in comparison to B(C$_6$F$_5$)$_3$-derived **1a** and doubly activated **1c**. It is also noteworthy that the colors of both **1a** and **1b** are a similar shade of bright yellow, whereas doubly activated **1c** has a deep red color.

Recently, relatively weak Lewis bases such as ethers and phosphines have been used to simulate incoming olefinic monomer units coordinating to metallocenium cations. Such experiments have provided information on the mechanism of anion displacement that must accompany olefin insertion[31] and the role that the anion plays after displacement.[20c] Similar experiments with **1a** and **1b** were attempted using THF as a Lewis base. Interestingly, while reaction of **1a** with THF cleanly displaces the H$_3$CB(C$_6$F$_5$)$_3^-$ anion forming the expected metallocenium THF adduct, the same reaction with **1b** results not in displacement of H$_3$CAl(C$_6$F$_5$)$_3^-$ but in regeneration of the parent dimethylmetallocene and formation of the THF−Al(C$_6$F$_5$)$_3$ adduct (eqs 3,4). Similar behavior of Al(C$_6$F$_5$)$_3$ with respect to other group 4 complexes has recently been reported by Chen and co-workers,[18a,28] and taken together these observations suggest qualitatively that Al(C$_6$F$_5$)$_3$ generally has significantly less affinity for methide than does B(C$_6$F$_5$)$_3$.

Structural Analysis of 1b and Comparisons to Other Ion Pairs. A comparison of important bond distances and angles for **1b**, averages of analogous H$_3$CB(C$_6$F$_5$)$_3^-$-containing metallocenium ion pairs, averages of relevant four-coordinate methyl borate and methyl aluminate compounds, metrical parameters for the diionic complex, *rac*-Me$_2$Si(η^5-indenyl)$_2$Zr^{2+} [H$_3$CAl(C$_6$F$_5$)$_3^-$]$_2$,[2b] the diionic complex, (^{t}Bu$_3$PN)$_2$Ti^{2+}[(CH$_3$)B(C$_6$F$_5$)$_3^-$]$_2$,[10] Me$_2$Si(Me$_4$Cp)(^{t}BuN)Ti(CH$_3$)$^+$H$_3$CB(C$_6$F$_5$)$_3^-$,[32] Me$_2$Si(Me$_4$Cp)(^{t}BuN)Ti(CH$_3$)$^+$H$_3$CB(C$_6$F$_5$)$_3^-$,[2b] and averages for neutral dimethyl zirconocenes are presented in Table 5 and represented graphically in Figure 3.[33,34]

It is evident from these data that the H$_3$CAl(C$_6$F$_5$)$_3^-$ anion of **1b** adopts a coordination geometry qualitatively similar to

(29) Siedle, A. R.; Newmark, R. A. *J. Organomet. Chem.* **1995**, *497*, 119−125.

(30) Synthesis of **1a** and **1c** in pentane only proceeds slowly and does not yield the desired ion pairs cleanly.

(31) Schaper, F.; Geyer, A.; Brintzinger, H.-H. *Organometallics* **2002**, *21*, 473.

(32) Fu, P. F.; Marks, T. J. Unpublished results.

Table 5. Comparison of Selected Bond Distances (Å) and Angles (deg) for Complex **1b**, for Averages of Four-Coordinate Anionic Aluminates and Borates,[35] for Averages of $B(C_6F_5)_3$ Adducts of Various Dimethyl Zirconocenes,[33] and for the Diionic Complexes *rac*-$(CH_3)_2Si(1\text{-indenyl})Zr^{2+}[(CH_3)_2Al(C_6F_5)_3^-]_2$,[2b] $(^tBu_3PN)_2Ti^{2+}[(CH_3)B(C_6F_5)_3^-]_2$,[10] $Me_2Si(Me_4Cp)(^tBuN)Ti(CH_3)^+(H_3C)B(C_6F_5)_3^-$,[32] $Me_2Si(Me_4Cp)(^tBuN)Ti(CH_3)^+(H_3C)Al(C_6F_5)_3^-$,[2b] $(Me_4Cp)_2Zr(CH_3)^+(H_3C)B(C_6F_5)_3^-$,[33e] and $(Me_4Cp)_2Zr(CH_3)^+(H_3C)B(C_6F_5)_3^-$ [33e]

Bond Distances (Å)

compound	E^a–CH_3	M^b–$(CH_3)_{brdg}$	M–$(CH_3)_{term}$
complex **1b**	2.026(4)	2.505(4)	2.252(3)
$L_2Zr(CH_3)^+ H_3CB(C_6F_5)_3^-$, average	1.675(6)	2.570(16)	2.251(7)
neutral dimethyl zirconocenes, average	–	–	2.277(4)
methyl aluminate compounds, average	1.998(4)	–	–
methyl borate compounds, average	1.640(2)	–	–
$(SBI)Zr^{2+}[(CH_3)Al(C_6F_5)_3^-]_2$	2.084(2)	2.431(2)	–
	2.059(2)	2.454(2)	–
$(^tBu_3PN)_2Ti^{2+}[(CH_3)B(C_6F_5)_3^-]_2$	1.687(11)	2.334(8)	–
$Me_2Si(Me_4Cp)(^tBuN)Ti(CH_3)^+(H_3C)B(C_6F_5)_3^-$	1.675(5)	2.364(3)	2.087(4)
$Me_2Si(Me_4Cp)(^tBuN)Ti(CH_3)^+(H_3C)Al(C_6F_5)_3^-$	2.033(3)	2.332(3)	2.097(3)
$(Me_4Cp)_2Zr(CH_3)^+(H_3C)B(C_6F_5)_3^-$	1.694(7)	2.600(5)	2.242(5)
$(Me_4Cp)_2Zr(CH_3)^+(H_3C)Al(C_6F_5)_3^-$	2.055(4)	2.258(3)	2.510(3)

Bond Angles (deg)

compound	E–CH_3–M	CH_3–M–CH_3
complex **1b**	160.3(2)	93.25(13)
$L_2Zr(CH_3)^+ H_3CB(C_6F_5)_3$, average	170(2)	91.8(12)
neutral dimethyl zirconocenes, average	–	95.6(6)
$(SBI)Zr^{2+}[(CH_3)Al(C_6F_5)_3^-]_2$	163.31(15)	105.68(8)
	169.67(12)	–
$(^tBu_3PN)_2Ti^{2+}[(CH_3)B(C_6F_5)_3^-]_2$	175.04	104.59
$Me_2Si(Me_4Cp)(^tBuN)Ti(CH_3)^+(H_3C)B(C_6F_5)_3^-$	170.2(2)	100.8(1)
$Me_2Si(Me_4Cp)(^tBuN)Ti(CH_3)^+(H_3C)Al(C_6F_5)_3^-$	169.03(16)	–
$(Me_4Cp)_2Zr(CH_3)^+(H_3C)B(C_6F_5)_3^-$	174.0(3)	90.84(18)
$(Me_4Cp)_2Zr(CH_3)^+(H_3C)Al(C_6F_5)_3^-$	177.2(2)	90.64(12)

[a] E = B, Al. [b] M = Zr, Ti.

those of zirconocenium $H_3CB(C_6F_5)_3^-$-containing ion pairs. The Zr−CH_3−Al bond angle is, as in the borane-derived ion pairs, nearly linear, and the CH_3−Zr−CH_3 bond angles are nearly identical at ∼93°. The Zr−$(CH_3)_{terminal}$ bond lengths are also essentially indistinguishable at ∼2.25 Å. However, the length of the Zr−$(CH_3)_{bridging}$ bond is significantly shorter for **1b** at 2.505(4) Å than the average of those seen for analogous $B(C_6F_5)_3$-derived zirconocenium ion pairs at 2.570(16) Å, reflecting less complete abstraction by $Al(C_6F_5)_3$ in comparison to $B(C_6F_5)_3$.

Comparing the metrical parameters for **1b** and the average metrical parameters for $B(C_6F_5)_3$-derived zirconocenium ion pairs with averages from neutral dimethyl zirconocenes, it can be seen that, upon $Al(C_6F_5)_3$ or $B(C_6F_5)_3$ coordination, the resulting Zr−$(CH_3)_{terminal}$ bond is shortened by about 0.025 Å in both cases. In addition, the resulting Zr−$(CH_3)_{bridging}$ bonds are significantly elongated versus the neutral metallocene Zr−CH_3 bonds. In the case of $Al(C_6F_5)_3$-derived **1b**, the Zr−$(CH_3)_{bridging}$ bond is about 0.23 Å longer, and in the case of $B(C_6F_5)_3$-derived zirconocenium ion pairs, the Zr−$(CH_3)_{bridging}$ bond is about 0.29 Å longer. The CH_3−Zr−CH_3 bond angle is moderately perturbed contracting from ∼95.6° to ∼91.8° for borane-derived ion pairs and to 93.3° for **1b**.

To better define the relative lengthening of the E−$(CH_3)_{bridging}$ bonds due to coordination by the metalloid center, an analysis of the crystal structures of four-coordinate anionic methylborate and methylaluminate compounds in which there is a terminal B−CH_3 or Al−CH_3 group was conducted.[35] The data indicate an average bond length of 1.640(2) Å for B−$(CH_3)_{terminal}$ bonds and 1.998(4) Å for Al−$(CH_3)_{terminal}$ bonds. In comparison, the average B−$(CH_3)_{bridging}$ bond length for $B(C_6F_5)_3$-derived zirconocenium ion pairs is 1.675(6) Å (0.035 Å, ∼2.1% longer), and the Al−CH_3 bond length for **1b** is 2.026(4) Å (0.028 Å, ∼1.4% longer). The extent of Al−CH_3 bond elongation induced by coordination of the bridging methide group to the zirconium center thus appears to be somewhat less than that observed for the $B(C_6F_5)_3$-derived ion pairs. Note that the difference in B−CH_3 vs Al−CH_3 elongation, 0.007 Å, is modest and falls within the dispersion of reported B−$(CH_3)_{bridging}$ bond lengths. However, this result, in conjunction with the observation that the Zr−$(CH_3)_{bridging}$ bond is significantly shorter for **1b**, argues for a less complete abstraction of methide from the zirconocenium center by $Al(C_6F_5)_3$ in comparison to $B(C_6F_5)_3$.

A direct comparison of the different methide-abstracting tendencies of $Al(C_6F_5)_3$ and $B(C_6F_5)_3$ can also be made by comparing the crystal structures of $Me_2Si(Me_4Cp)(^tBuN)Ti(CH_3)^+H_3CB(C_6F_5)_3^-$[32] and $Me_2Si(Me_4Cp)(^tBuN)Ti(CH_3)^+H_3CAl(C_6F_5)_3^-$.[2b] Here we see more evidence that $Al(C_6F_5)_3$ does not abstract methide as completely as $B(C_6F_5)_3$. The Ti−

(33) The cationic portions of the metallocenium ion pairs used for structural parameter averaging are as follows: (a) [(1,2-$Cp_2(C_2H_4)$)$ZrCH_3^+$)] Beck, S.; Prosenc, M.-H.; Brintzinger, H.-H.; Goretzki, R.; Herfert, N.; Fink, G. *J. Mol. Catal. A: Chem.* **1996**, *111*, 67. (b) [$Cp_2ZrCH_3^+$] Guzei, I. A.; Stockland, R. A.; Jordan, R. F. *Acta Crystallogr., Sect. C: Cryst. Struct. Commun.* **2000**, *56*, 635. (c) [(1,2-$(CH_3)_2Cp)_2ZrCH_3^+$] ref 3b. (d) [Me_2Si-(2-CH_3-4-^{t}BuCp)$_2ZrCH_3^+$] ref 33a. (e) [$((CH_3)_4Cp)_2ZrCH_3^+$] Lui, Z.; Somsook, E.; Landis, C. R. *J. Am. Chem. Soc.* **2001**, *123*, 2915. (f) [(Me_5-Cp)$_2$Zr CH_3^+, (1,3-$TMS_2Cp)_2ZrCH_3^+$] ref 3a. (h) [$(CH_3)_2C$(Cp)(Flu)$ZrMe^+$] ref 5a.

(34) The average bond lengths and angles presented here have been computed by averaging analogous bonds across all of the relevant structures found within the Cambridge Crystallographic Data Centre database. The standard deviations reported are calculated by the method of Taylor et al: Taylor, B.; Kennard, O. *J. Chem. Inf. Comput. Sci.* **1986**, *26*, 28.

(35) Examples of some of the borate anions surveyed: Me_4B^-, $MePh_3B^-$, Me_2-(2-pyridyl)$_2B^-$. Examples of some of the aluminate anions surveyed: Me_4Al^-, (adamantyl)$_2Me_2Al^-$, $Me_3(CN)Al^-$. For a complete listing of the crystal structures surveyed, see Supporting Information.

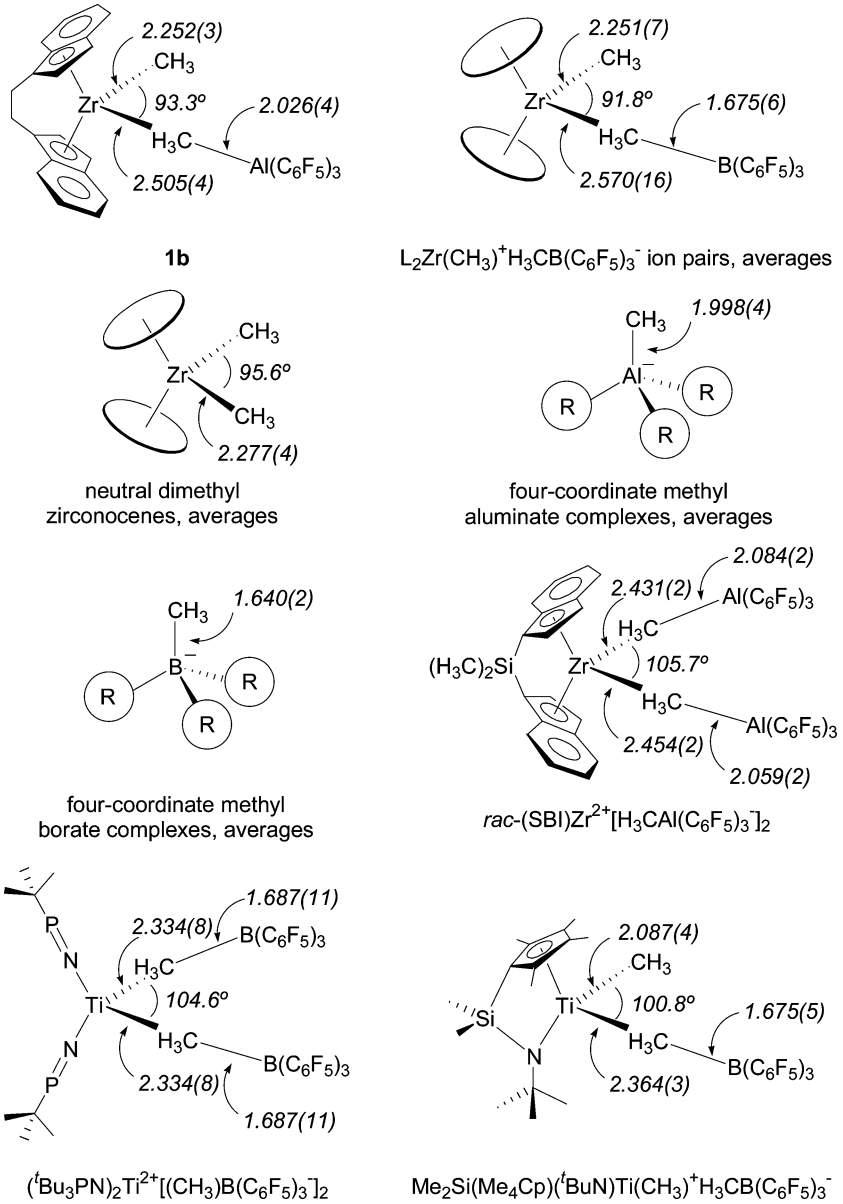

Figure 3. Comparison of relevant metrical parameters for ion pair **1b**, for averages of $L_2Zr(CH_3)^+H_3CB(C_6F_5)_3^-$ ion pairs, for averages of neutral dimethyl zirconocenes, for averages of four-coordinate aluminate and borate complexes, for $(SBI)Zr^{2+}[H_3CAl(C_6F_5)_3^-]_2$, and for $(^tBu_3PN)_2Ti^{2+}[H_3CB(C_6F_5)_3^-]_2$.

$(CH_3)_{brdg}$ bond length is shorter in the alane complex by 0.032 Å (2.364(3) Å vs 2.332(3) Å), and the Ti−$(CH_3)_{term}$ bond length is longer in the alane complex by 0.010 Å (2.087(4) Å vs 2.097-(3) Å), consistent with the bridging methyl being more tightly bound to the Ti center in $Me_2Si(Me_4Cp)(^tBuN)TiCH_3^+H_3CAl(C_6F_5)_3^-$. This same trend holds true for the two analogous compounds $(Me_4Cp)_2Zr(CH_3)^+(H_3C)Al(C_6F_5)_3^-$ and $(Me_4Cp)_2Zr(CH_3)^+(H_3C)B(C_6F_5)_3^-$.[33e] Here again we see a shortening of the Zr−$(CH_3)_{brdg}$ bond of the Al compound versus the B compound (2.510(3) Å vs 2.600(5) Å) and a lengthening of the Zr−$(CH_3)_{term}$ bond (2.258(3) Å vs 2.242(5) Å). Thus it seems to be a general phenomenon that $Al(C_6F_5)_3$ abstracts the bridging methide less fully away from the metal center than $B(C_6F_5)_3$.

In comparing diionic *rac*-$Me_2Si(\eta^5\text{-indenyl})_2Zr^{2+}[H_3CAl(C_6F_5)_3^-]_2$ with **1b**, note that the Zr−$(CH_3)_{bridging}$ bonds are significantly shorter at 2.431(2) Å and 2.454(2) Å in the former complex versus 2.505(4) Å in ion pair **1b**. The 2.084(2) Å and 2.059(2) Å Al−$(CH_3)_{bridging}$ bond lengths of the diionic complex are also significantly longer than the Al−$(CH_3)_{bridging}$ bond of **1b**, 2.026(4) Å. These parameters are consistent with significantly less abstractive character in the individual Zr−H_3C−Al linkages of the bis-$Al(C_6F_5)_3$ adduct. The CH_3−Zr−CH_3 angle of 105.68(8)° in *rac*-$Me_2Si(\eta^5\text{-indenyl})_2Zr^{2+}[H_3CAl(C_6F_5)_3^-]_2$ is 12.4° wider than that of **1b**, which likely reflects repulsive nonbonded interactions between the two $Al(C_6F_5)_3$ moieties. Indeed, analysis of the nonbonding interactions between the two closest C_6F_5 groups from the different $Al(C_6F_5)_3$ moieties using the published coordinates[2b] and PLATON crystal structure analysis software[36] indicates several interatomic contacts near the sum of the corresponding van der Waals radii (i.e., F1−F26, 2.989(3) Å; F26−C24, 3.132(3) Å; F27−C26, 3.267(4) Å; the sums of van der Waals radii are 2.94 Å and 3.17 Å for F···F and C···F, respectively). Thus, the second methide abstraction by $Al(C_6F_5)_3$ apparently creates a sterically crowded environment about the zirconocenium center, which appears to weaken the first Al−CH_3 bond and overall results in both

(36) Spek, A. L. *J. Appl. Crystallogr.* **2003**, *36*, 7.

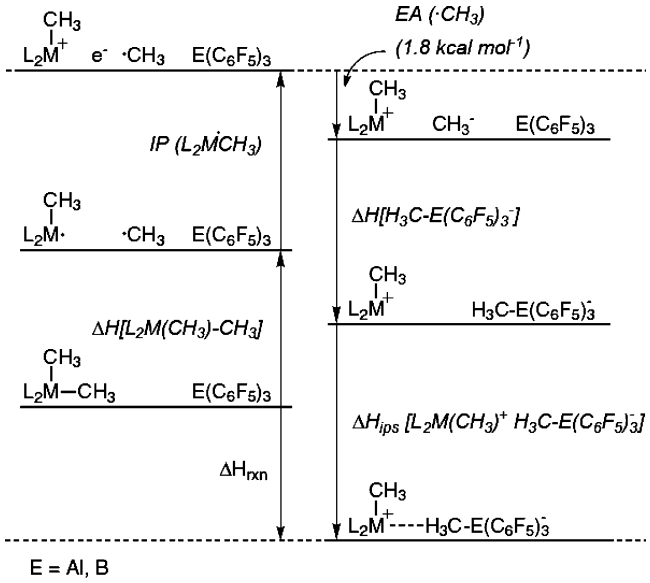

Figure 4. Approximate thermodynamic cycle for the formation of $L_2MCH_3^+$ $H_3CE(C_6F_5)_3^-$ ion pairs from neutral metallocene and $E(C_6F_5)_3$ (E = B, Al) precursors.

methide moieties being less completely abstracted than in the monoionic case. The ability of the d^0 zirconium center to stabilize an additional formal positive charge resulting from a second methide abstraction may also be a contributing factor.

It is instructive to briefly compare the metrical parameters of $(^tBu_3PN)_2Ti^{2+}[H_3CB(C_6F_5)_3^-]_2$[10] with those of *rac*-$Me_2Si(\eta^5$-indenyl$)_2Zr^{2+}[H_3CAl(C_6F_5)_3^-]_2$. The $^tBu_3PN$ ligands of $(^tBu_3PN)_2Ti^{2+}[H_3CB(C_6F_5)_3^-]_2$ afford a significantly less sterically hindered environment around the metal center than do multihapto metallocene-type π-ligands. Like *rac*-$Me_2Si(\eta^5$-indenyl$)_2Zr^{2+}[H_3CAl(C_6F_5)_3^-]_2$, $(^tBu_3PN)_2Ti^{2+}[H_3CB(C_6F_5)_3^-]_2$ has a $(CH_3)_{bridging}-M-(CH_3)_{bridging}$ bond angle of about 105°. There are also close contact nonbonding interactions between the two closest C_6F_5 groups from the different $B(C_6F_5)_3$ moieties which are significantly shorter than the sum of the fluorine van der Waals radii (i.e., F15···F15a, 2.835(6) Å). Note also that the structural parameters associated with $Me_2Si(Me_4Cp)(^tBuN)Ti(CH_3)^+H_3CB(C_6F_5)_3^-$, a sterically "open" titanium complex with only a single coordinated $B(C_6F_5)_3$ group, are indicative of less steric crowding: the CH_3-M-CH_3 angle is 3.7° narrower at 100.8(1)°, and the $B-CH_3$ bond length is also shorter at 1.650(5) Å.

Although the differing ligand sets and metal ions rule out a completely rigorous structural comparison of the bisborane and bisalane complexes, the data suggest that two $B(C_6F_5)_3$ moieties must suffer significant steric crowding to effect the abstraction of two methides and that this behavior is unfavorable in more sterically congested metallocene alkyl systems.

Thermodynamics of Methide Abstraction. The calorimetric results for a series of methide abstraction experiments (Table 3) indicate that in toluene, methide abstraction by $Al(C_6F_5)_3$ is approximately 8 kcal mol^{-1} less exothermic than by $B(C_6F_5)_3$. This result stands in variance to the DFT prediction that abstraction by $Al(C_6F_5)_3$ should be more exothermic.[13] If the data are considered in terms of an approximate thermodynamic cycle (Figure 4), the difference in methide abstraction enthalpy between $B(C_6F_5)_3$ and $Al(C_6F_5)_3$ must arise from some combination of differences in ion pair separation enthalpy (ΔH_{ips}) or in the methide affinity of the cocatalyst (ΔH_{E-Me}). As the borate and aluminate anions are of similar shape and coordination, and the interactions with the zirconocenium cation are predominantly electrostatic,[21c,d] it is a reasonable assumption that the ion pair separation energies are roughly similar. Thus, the difference in methide abstraction enthalpies would result primarily from the smaller methide affinity of $Al(C_6F_5)_3$ versus $B(C_6F_5)_3$. This conclusion is in agreement with the observed substantially lower apparent Lewis acidity of $Al(C_6F_5)_3$ with respect to benzonitrile.[12] Nevertheless, regardless of how the energetics are partitioned, it is clear that the reaction with the alane is substantially less exothermic.

Cowley and co-workers have reported that $Al(C_6F_5)_3$ can be crystallized as a 1:1 benzene or toluene adduct to afford a product structurally reminiscent of isoelectronic silylium arene adducts[8] (**D**) and that this structure persists in solution to the extent that it is observable in ^{1}H NMR splitting patterns. To

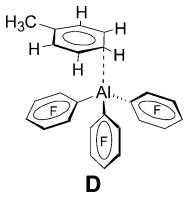

D

the best of our knowledge, this behavior has not been observed for $B(C_6F_5)_3$. Thus, one consideration that should not be ignored is the possibility that the $Al(C_6F_5)_3$ enthalpy of toluene solvation/coordination is greater than that of $B(C_6F_5)_3$ and that measured $Al(C_6F_5)_3$ metallocene methide abstraction enthalpies are influenced by the arene decomplexation that must formally precede methide abstraction. In the literature, $Al(C_6F_5)_3$ is typically formulated as $Al(C_6F_5)_3\cdot(C_7H_8)_{0.5}$ when prepared from toluene and dried in vacuo.[12,25] Indeed, quantification of the toluene content in the $Al(C_6F_5)_3$ used in the present work using ^{1}H NMR with ferrocene as an internal standard indicates a toluene/$Al(C_6F_5)_3$ ratio of ~0.55.

The enthalpies of solvation, as measured by a simple batch addition calorimetry experiment, indicate the heat of solvation of $B(C_6F_5)_3$ to be +5.5(3) kcal mol^{-1} and that of $Al(C_6F_5)_3\cdot(C_7H_8)_{0.5}$ to be +2.9(1) kcal mol^{-1} (both endothermic). The signs and magnitudes of these parameters are well within the range of solvation enthalpies previously reported for organotransition metal complexes of these dimensions and molecular masses.[37] That the solvation of $Al(C_6F_5)_3\cdot(C_7H_8)_{0.5}$ is only 2.6 kcal mol^{-1} less endothermic than that of $B(C_6F_5)_3$ indicates that solvation effects are not likely to contribute greatly to the overall ion pair formation enthalpies measured. The potentially explosive nature of $Al(C_6F_5)_3$ precludes attempting to prepare a completely toluene-free sample. However, if it is assumed that the 2.6 kcal mol^{-1} ΔH_{solv} difference for $Al(C_6F_5)_3$ versus $B(C_6F_5)_3$ results primarily from 1:1 $Al(C_6F_5)_3-$toluene adduct formation, then the heat of formation of such adducts must at most account for only a few kcal mol^{-1} ($\lesssim 2 \times 2.6$ kcal mol^{-1}), insufficient to account entirely for the significantly less exothermic ion pair formation enthalpy associated with $Al(C_6F_5)_3$ versus $B(C_6F_5)_3$. Furthermore, the derived thermochemical quantities represent an accurate measure of the "in situ" reaction energetics in the

(37) (a) Schock, L. E.; Marks, T. J. *J. Am. Chem. Soc.* **1988**, *110*, 7701. (b) Nolan, S. P.; Stern, D.; Marks, T. J. *J. Am. Chem. Soc.* **1989**, *111*, 7844.

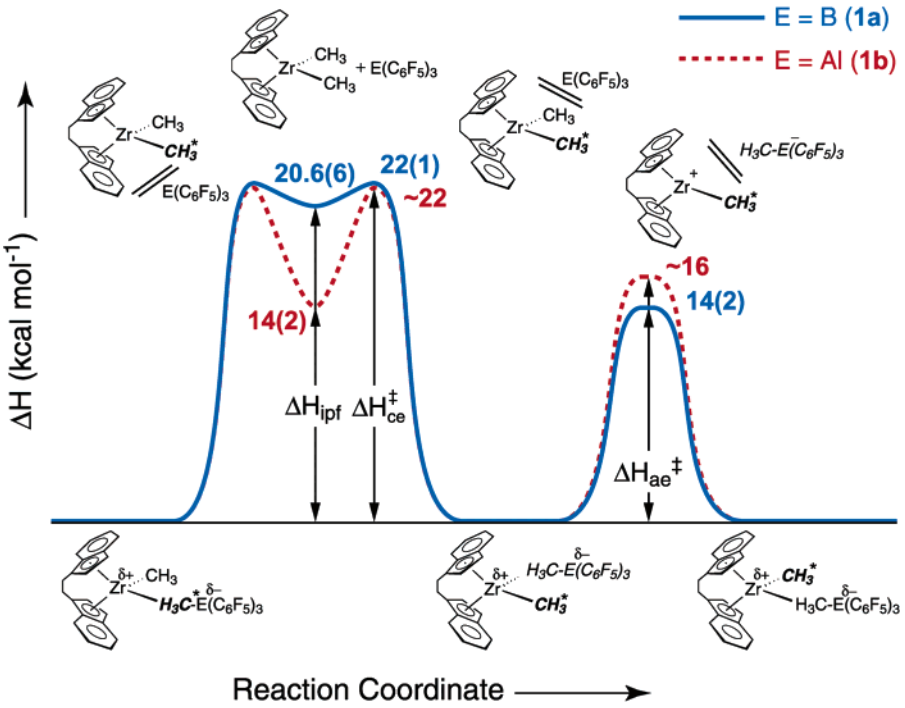

Figure 5. Schematic representation of reaction coordinates for formation and structural reorganization of **1a** and **1b**.

medium where such activators are frequently used. It is conceivable that desolvation of $Al(C_6F_5)_3 \cdot (C_7H_8)_x$ contributes entropically to adduct formation.

The second methide abstraction by $Al(C_6F_5)_3$ is only modestly exothermic at $\Delta H_{ipf} = -2$ to -4 kcal mol^{-1} (Table 3). This significant attenuation in methide abstraction enthalpy likely results from steric crowding of the two $H_3CAl(C_6F_5)_3^-$ moieties around the metal center and consequent weakening of the first methide abstractive bond as well as from the limited ability of the d^0 zirconium metal center to accommodate additional formal positive charge. The shorter $Zr-(CH_3)_{bridging}$ bonds and longer $Al-(CH_3)_{bridging}$ bonds for *rac*-$Me_2Si(\eta^5$-indenyl$)_2Zr^{2+}[H_3CAl(C_6F_5)_3^-]_2$ observed after a second methide abstraction are indicative of a weakening of the first $Al-(CH_3)_{bridging}$ bond and a strengthening of the $Zr-(CH_3)_{bridging}$ bond, which as the microscopic reverse of the first methide abstraction, likely makes an endothermic contribution. Furthermore, the significantly diminished solubility of complex **1c** in comparison to complex **1b** suggests that **1c** may be considerably more polar. This greater polarity would therefore reflect greater positive charge density accumulation on the zirconium center which also is an endothermic process.

It has been argued by Park and co-workers by measurement of benzonitrile adduct stretching frequencies that $B(C_6F_5)_3$ is more Lewis acidic than $Al(C_6F_5)_3$.[12] Although there is not a large literature on the Lewis acidities of aryl aluminum compounds, there are a number of studies in which boron compounds have been shown to be more Lewis acidic than their aluminum homologues.[38] For example, BCl_3 is found to be more Lewis acidic than $AlCl_3$ by most experimental measurements on 9-fluorenone adducts (i.e., IR, UV−vis, and NMR experiments)[38e] as well as NMR assays of Lewis acidity using aldehydes, ketones, esters, and nitriles.[38b] A possible exception to this trend comes from X-ray diffraction analyses of adducts of AlX_3 and BX_3 (X = halide) 9-fluorenone: derived Al−O and $O-C_{(fluorene)}$ bond distances indicate the opposite acidity trends.[38e] This observation possibly accounts for the comparatively little difference between the relative $Al-CH_3$ and $B-CH_3$ bond lengths in the present work despite other evidence indicating a weaker Lewis acidity and methide affinity of $Al(C_6F_5)_3$.

Finally, if the reduced enthalpy of methide abstraction exhibited by $Al(C_6F_5)_3$ is a result of a weaker Lewis acidity, the less anionic nature of the $H_3CAl(C_6F_5)_3^-$ anion should be reflected in ^{19}F NMR spectral parameters.[39,40] The *o*-F and *p*-F resonances of $Al(C_6F_5)_3$-derived **1b** are shifted downfield from the *m*-F resonance by 39.0 and 8.2 ppm, respectively, in comparison with only 30.8 and 5.1 ppm, respectively, for **1a**. This relative chemical shift difference of 8.2 ppm for the *o*-F resonance and 3.1 ppm for the *p*-F resonance in relation to the *m*-F resonance is a strong indicator[39,40] of less anionic C_6F_5 character in the $H_3CAl(C_6F_5)_3^-$ moiety. Note that the *o*-F, *p*-F vs *m*-F parameters for **1c** of 37.7 and 9.3 ppm, respectively, are also in accord with diminished anionic character.

Dynamics of Anion Exchange. The kinetic parameters determined for ion pair structural dynamics, as defined by eqs 5 and 6, are understandable in terms of previous measurements on analogous complexes (Table 4).[20a] For $B(C_6F_5)_3$-derived complex **1a**, the enthalpic barriers to anion exchange and cocatalyst exchange are 14 kcal mol^{-1} and 22 kcal mol^{-1}, respectively. The reaction coordinates defined by these data along with the ion pair formation enthalpy data are illustrated schematically in Figure 5. Note that the kinetic parameters are essentially unchanged over a 5-fold concentration range, consistent with a predominantly unimolecular exchange mechanism under these conditions.

(38) (a) Lappert, M. F. *J. Chem. Soc.* **1962**, 542. (b) Childs, R. F.; Mulholland, D. L.; Nixon, A. *Can. J. Chem.* **1982**, *60*, 801. (c) Laszlo, P.; Teston, M. *J. Am. Chem. Soc.* **1990**, *112*, 8750. (d) *Group 13 Chemistry*; Shapiro, P. J., Atwood, D. A., Eds.; ACS Symposium Series 822; American Chemical Society: Washington, DC, 2002. (e) Branch, C. S.; Bott, S. G.; Barron, A. R. *J. Organomet. Chem.* **2003**, *666*, 23.
(39) Parshall, G. W. *J. Am. Chem. Soc.* **1966**, *88*, 704.
(40) Chen, E. Y.-X.; Marks, T. J. *Chem. Rev.* **2000**, *100*, 1391.

Although the exact mechanism by which translation of the anion from one side of the metallocene framework to the other occurs is not completely defined,[41] the activation energetics for these exchanges must depend on the energetics which bind the bridging methide group to the metal center. When the $Zr^+\cdots H_3CE(C_6F_5)_3^-$ interaction is relatively weak (ionic), the barrier to anion exchange (eq 5) should be relatively low. As illustrated in Figure 5, the barrier to anion separation/exchange is ~2 kcal mol^{-1} greater for $Al(C_6F_5)_3$-derived **1b** than for $B(C_6F_5)_3$-derived **1a** (at 72 °C, k_{ae} is ~10× less), consistent with this picture. Although data are not available over the full range of line shapes, the general trend is informative, and the results are consistent with the model suggested by the thermochemical data: $Al(C_6F_5)_3$ has significantly less affinity for methide than does $B(C_6F_5)_3$; thus, the $Zr-(CH_3)_{bridging}$ bond is stronger for **1b** than for **1a**, resulting in a higher anion exchange barrier for $Al(C_6F_5)_3$-derived **1b** than for $B(C_6F_5)_3$-derived **1a**. While the same lines of argument would make the case that $\Delta H^{\ddagger}_{ce}$ for **1b** should be less than that for **1a**, the accuracy of the data only permits us to suggest that this is probably the case. At 72 °C, k_{ce} is 10% greater for **1b**.

Conclusions

The results presented here are all consistent with a model in which $Al(C_6F_5)_3$ exhibits significantly less Lewis acidity than $B(C_6F_5)_3$, particularly in terms of methide abstraction tendency. The structural, thermochemical, and structural dynamic observations are consistent with reduced polarization of the $Zr-CH_{3(bridging)}$ bond and an overall less complete methide abstraction by $Al(C_6F_5)_3$ in comparison to $B(C_6F_5)_3$. The ability of $Al(C_6F_5)_3$ to abstract two methide groups from group 4 metallocenes, unlike $B(C_6F_5)_3$, seems most likely due to the larger covalent radius of aluminum, which better accommodates the steric crowding of two $Al(C_6F_5)_3$ moieties around the metal center.

The chemical and physical differences between $Al(C_6F_5)_3$ and $B(C_6F_5)_3$ reported here relate directly to product polymer microstructure. In general, the greater the cationic character induced by the cocatalyst at the metal center, the greater the activity for polymerization.[2,5,6,40] We find that the propylene polymerization activity of the $Al(C_6F_5)_3$-activated Me_2C(Fluorenyl)(Cp)$Zr(CH_3)_2$ catalyst is ~10 × less than that of the analogous $B(C_6F_5)_3$-activated catalyst.[6] Furthermore, recent studies have shown that the syndiotacticity of polypropylene produced by Me_2C(Fluorenyl)(Cp)$Zr(CH_3)_2$-based catalysts is strongly modulated by the coordinative tendencies of the counteranion.[5a,42] The mechanism by which syndiotacticity is encoded by C_s-symmetric catalysts relies on the growing polymer chain migrating from one side of the metallocene framework to the other (analogous to eq 5) during each monomer enchainment event, with stereoerrors introduced when the polymer chain exchanges sides faster than the rate of concurrent monomer enchainment. This migration has been shown to be strongly attenuated by more strongly coordinating anions.[5a] The syndiotacticity of polypropylene produced by $Al(C_6F_5)_3$-activated Me_2C(Fluorenyl)(Cp)$Zr(CH_3)_2$ is ~16% greater than for the $B(C_6F_5)_3$-activated catalyst.[6b] These observations are consistent with the less complete methide abstraction and smaller k_{ae} associated with the $Al(C_6F_5)_3$ cocatalyst (see Figure 5).

Taken together, all of the current results as well as those from polymerization studies[5a,42] are consistent with a picture of $Al(C_6F_5)_3$ displaying less Lewis acidity and less methide affinity than $B(C_6F_5)_3$. $Al(C_6F_5)_3$ has already been shown to have application in a large number of polymerization environments. It is likely efforts to extend its utility further will be forthcoming from various laboratories, and the current observations presented here may help to guide those efforts.

Acknowledgment. We thank the US DOE (Grant DE-FG 02-86 ER13511) for financial support of this work. We also thank Dr. C. Zuccaccia, Mr. J. A. Roberts, and Dr. M.-C. Chen for helpful discussions.

Supporting Information Available: Literature-derived values used to calculate average structural parameters and NMR spectra. Crystallographic data for **1b** in CIF format. These materials are available free of charge via the Internet at http://pubs.acs.org.

JA0429622

(41) It has been suggested that anion side exchange occurs via ion pair aggregates: (a) ref 20b. However, this suggestion is not supported by measurements of ion pair aggregation at these concentrations: (b) ref 20c. (c) Stahl, N. G.; Zuccaccia, C.; Jensen, T. R.; Marks, T. J. *J. Am. Chem. Soc.* **2003**, *125*, 5256. Aggregation effects are also not observable in polymerization experiments: (d) ref 5a. Recent evidence indicates that impurities may be the source of observed intermolecular exchange processes: (e) Beringhelli, T.; Alfonso, G. D.; Maggioni, D.; Mercandelli, P.; Sironi, A. *Chem.—Eur. J.* **2005**, *11*, 650.

(42) Mohammed, M.; Nele, M.; Al-Humydi, A.; Xin, S.; Stapleton, R. A.; Collins, S. *J. Am. Chem. Soc.* **2003**, *125*, 7931.